molecular pharmaceutics

Article

pubs.acs.org/molcularpharmaceutics

Interaction between Cell-Penetrating Peptides and Acid-Sensitive Anionic Oligopeptides as a Model for the Design of Targeted Drug Carriers

Chunmeng Sun,[†,‡] Wei-Chiang Shen,[‡] Jiasheng Tu,*[,†] and Jennica L. Zaro*[,‡]

[†]State Key Laboratory of Natural Medicines, Department of Pharmaceutics, School of Pharmacy, China Pharmaceutical University, 24 Tong Jia Xiang, Nanjing 210009, China

[‡]Department of Pharmacology and Pharmaceutical Science, University of Southern California, 1985 Zonal Ave, Los Angeles, California 90033, United States

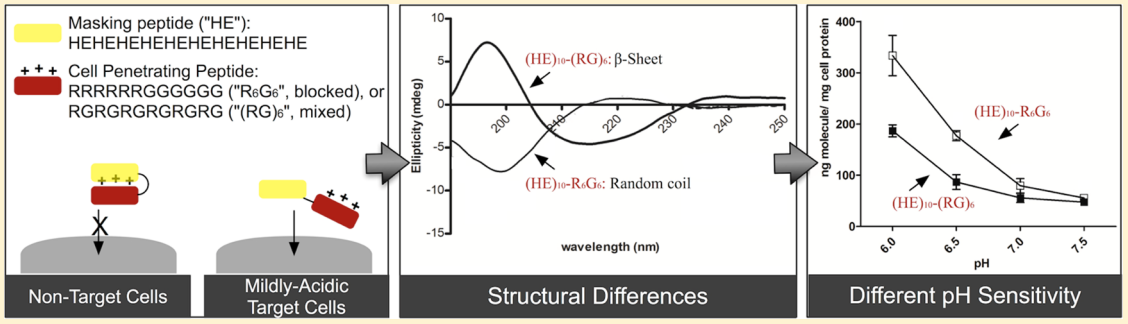

ABSTRACT: Overcoming the nonspecific cellular uptake of cell-penetrating peptides (CPPs) is a major hurdle in their clinical application. Using pH as the activation switch, histidine-glutamic acid (HE) dipeptide repeats were fused to CPPs to trigger the membrane-penetrating activity at mildly acidic pH environments (i.e., pH 6.5 or below) while masking the internalization at neutral pH (i.e., pH 7.0 or above). In this study, a series of recombinant GST-fusion proteins containing an HE oligopeptide sequence (i.e., $(HE)_n$ with n = 8, 10, or 12) and a cationic CPP (i.e., $YG(RG)_6$, YGR_6G_6, or Tat) were engineered for a pH-sensitive study comparing their cellular uptake and surface binding in cultured HeLa cells. Circular dichroism (CD) spectroscopy was performed to correlate differences between CPPs in secondary structure with the pH sensitivity. YGR_6G_6 with clustered arginine residues exhibited greater pH sensitivity in cellular uptake than $YG(RG)_6$ with separated arginine residues. Increasing the stretch of HE repeats decreased cellular uptake and surface binding for both $YG(RG)_6$ and YGR_6G_6. The ratio of cellular internalization at pH 7.5 vs 6.0 was not changed by the presence of serum. CD spectral data revealed that both $(HE)_{10}$-Tat and $(HE)_{10}$-YGR_6G_6 exhibited an unordered secondary structure, whereas $(HE)_{10}$-$YG(RG)_6$ adopted an antiparallel β-sheet conformation. This β-sheet conformation presumably stabilized the association of $(HE)_{10}$ with $YG(RG)_6$, leading to weakened pH sensitivity of $(HE)_{10}$-$YG(RG)_6$. On the other hand, the random-coiled structures, that is, $(HE)_{10}$-YGR_6G_6 and $(HE)_{10}$-Tat, both showed higher pH sensitivity as determined in cell experiments. The data presented in this study provide a basis for the future design of pH-sensitive HE-CPP carrier for targeted drug delivery.

KEYWORDS: *cell-penetrating peptide, arginine-rich peptide, pH sensitive delivery, circular dichroism*

INTRODUCTION

Rational utilization of the power of cell-penetrating peptides (CPPs) has been pursued for decades since HIV's trans-activator of transcription (Tat) protein joined the fascinating family as the first unveiled CPP model.[1] CPPs, also known as protein transduction domains (PTDs) or membrane transduction peptides (MTPs), generally consist of 30 or less amino acids and are categorized as amphipathic or cationic depending on their sequences. Receptor-independent internalization and noninvasive entry into cells are the two major advantages that draw increasing attention to the field of CPP-based intracellular delivery systems. A variety of cargos, including bioactive molecules,[2,3] DNA/siRNA,[4,5] quantum dots,[6] and nanoparticles,[7,8] have been delivered using different types of CPPs *in vitro* and *in vivo*. Additionally, some studies have shown that CPPs could also promote gastrointestinal absorption of protein drugs[9,10] as well as direct brain delivery via intranasal administration.[11]

However, lack of specificity is the major challenge for CPPs to be employed clinically.[12−14] Many approaches have been investigated to confer CPPs with the ability of targeting delivery, but no break-through technology has yet been achieved. The nonspecific *in vivo* biodistribution of CPPs is

Received: December 13, 2013
Revised: February 24, 2014
Accepted: April 3, 2014
Published: April 3, 2014

mostly caused by the cationic characteristics of the oligopeptide.[15] Therefore, one of the most promising approaches is to reversibly mask the positive charges in a CPP with a polyanionic counterpart. The selective activation of oligoanion-masked CPP can be achieved by specific proteolysis,[16] light activation[17] or differences in the microenvironment[18] at target site. Recently, we have designed a recombinant co-oligopeptide containing Model Amphipathic Peptide (MAP, KLALKLALKALKAALKLA) as the CPP sequence, and 10-mer of histidine-glutamic acid repeats ($(HE)_{10}$) as a pH-sensitive blocking oligopeptide. MAP is an amphipathic peptide that shows high cellular uptake and exhibits an α-helical structure. This recombinant construct, "GST-HE-MAP", was highly pH-sensitive and could be activated under mildly acidic pH conditions. In cultured HeLa cells, it exhibited a low surface binding and cellular internalization at pH 7.4 but high surface binding and cellular internalization at pH 6.8 or below.[19] Furthermore, the construct showed high accumulation and retention for up to 24 h near the tumor site in a xenograft breast cancer mouse model.[20] In addition to solid tumor tissues, endosomal/lysosomal compartments[21] as well as the infectious/inflammatory sites[22] are also implicated as potential drug delivery targets with acidic bioenvironments. By conjugating with a ligand, HE-CPP under an inactive form at physiological pH could be internalized into target cells via a receptor-mediated endocytic pathway, thereby being activated in the endosomal or lysosomal compartments.[19] Similar to extracellular pH conditions in tumor tissues, the acidic microenvironments at the sites of infection or inflammation could weaken the masking effect of HE repeats, leading to restoration of the membrane-permeability of the CPP.

In this study, the systematic design of anionic oligopeptides for neutralizing the cationic charges in oligoarginine CPPs is investigated. Oligoarginine exhibits many differences from amphipathic CPPs like MAP, such as different intracellular localization,[23] and lacks a secondary structure.[24] Therefore, we wanted to determine if the same pH-sensitive masking sequence used on an amphipathic CPP could also be applied to cationic CPPs. The efficiency of masking and reactivation of CPPs may be influenced by many factors, such as the number of the positively charged amino acids in CPP, the polyanionic oligopeptide sequences, linker cleavability, and the location of the CPP and the masking sequences. In addition, the cationic charge distribution of the CPP, either as clustered or evenly mixed sequence, may also affect the neutralizing efficiency.[25] Using HE oligopeptide with various lengths, the masking effect on oligoarginine at a pH range between 6.0 and 7.5 was evaluated for the design of activatable CPPs with either clustered or mixed positive charges in the oligopeptides.

EXPERIMENTAL SECTION

Plasmid Construction and Production of Protein. The pGEX-4T-1 vectors (GE Healthcare Life Sciences, Piscataway, NJ) were utilized in this study to clone all plasmids. Similar to our previous design,[19] the fusion protein contains glutathione S-transferase (GST) as a protein cargo fused to an HE oligopeptide sequence ($(HE)_n$, n = 8, 10, or 12), a short pentaglycine linker (G_5), and a arginine-rich CPP ($YG(RG)_6$, YGR_6G_6, or Tat peptide (YGRKKRRQRRR)). In order to allow for further characterization of the HE-CPP peptide sequences, a tyrosine residue was incorporated in the CPP sequence for quantitation, while a thrombin cleavage recognition sequence (Leu-Val-Pro-Arg-Gly-Ser, LVPR$^{\downarrow}$GS) was reserved between GST and HE oligopeptide. The ssDNAs of $(HE)_n$ (n = 8, 10, and 12), G_5-$YG(RG)_6$ and G_5-YGR_6G_6 were synthesized by ValueGene Inc. (San Diego, CA). After annealing ssDNAs into dsDNA, the dsDNAs coding for $(HE)_n$ (n = 8, 10, or 12) and G_5-$YG(RG)_6$ or G_5-YGR_6G_6 were successively introduced into the pGEX-4T-1 vector downstream from the amino-terminal of GST sequence through BamH I, EcoR I, and Not I restriction enzyme cleavage sites. Due to the two-step clones and the EcoR I restriction enzyme cleavage site, an extra amino acid residue, phenylalanine (Phe, F), was present between the HE sequence and G_5 linker. After ligation and transformation, colony PCR was performed, and then plasmids were duplicated overnight in *Escherichia coli* (*E. coli*) DH5α competent cells in lysogeny broth (LB) media containing 75 μg/mL ampicillin and 20 mM L-Glucose at 37 °C. After sequencing (GeneWiz, San Diego, CA), the plasmids were transformed into *E. coli* expression strain BL21. The recombinant protein was expressed and purified using glutathione (GSH) agarose beads as the procedure described in our published report.[19] Samples collected during purification were analyzed by SDS-PAGE followed by Coomassie blue staining. The recombinant proteins produced for this study are listed in Table 1.

Table 1. Yield and Purity of Recombinant GST-Fusion Proteins

oligopeptide sequence	M.W. (kDa)	Yield[a] (mg)	pI[b]
GST-$(HE)_8EFG_5YG(RG)_6$	30.15	49.4	6.77
GST-$(HE)_{10}EFG_5YG(RG)_6$	30.68	43.5	6.62
GST-$(HE)_{12}EFG_5YG(RG)_6$	31.22	25.5	6.53
GST-$(HE)_8EFG_5YGR_6G_6$	30.15	40.9	6.77
GST-$(HE)_{10}EFG_5YGR_6G_6$	30.68	39.1	6.62
GST-$(HE)_{12}EFG_5YGR_6G_6$	31.22	21.1	6.53
GST-$(HE)_{12}EFG_5$YGRKKRRQRRR	31.48	15.8	6.71
GST-$(HE)_{10}$	30.34	39.7	6.20

[a]Amount per 500 mL LB media. The purity was >90% for all preparations, as determined by band density comparison in SDS-PAGE with Coomassie blue staining. [b]Isoelectric point (pI), calculated using an online software program[40]

Iodination of Protein. The purified recombinant GST-fusion proteins were radiolabeled with Na−^{125}I (PerkinElmer Health Sciences, Chicago, IL) using the chloramine T method as previously described.[26] ^{125}I-protein was purified by size exclusion chromatography using a gravity-flow column packed with Sephadex G50 beads (GE Healthcare Life Sciences). Reaction solution was loaded on the column prebalanced with PBS, and liquid flow-through was collected in fractions and monitored by measuring the radioactivity. Finally, fraction(s) containing ^{125}I-proteins were stored at −20 °C until use.

Cellular Uptake and Surface Binding Assay. Human cervical carcinoma (HeLa) cells were originally maintained at 37 °C in a 95% humidified atmosphere of 5% CO_2 in RPMI 1640 medium (Mediatech, Manassas, VA) supplemented with 10% fetal bovine serum (FBS), 2 mM L-glutamine, 50 U/mL penicillin and 50 μg/mL streptomycin. Two or three days before cellular uptake and surface binding assay, appropriate number of HeLa cells was seeded into 6-well plates. After being grown to confluence, cell monolayers were treated with serum-free or serum-containing (1−10% FBS) medium for 10 min followed by incubation in serum-free or serum-containing (1−10% FBS) medium at pH 6.0, 6.5, 7.0, or 7.5 containing 5 μg/

mL ^{125}I-labeled protein and protease inhibitor cocktail.[25] After 1 h of treatment at 37 °C, the cell monolayers were washed three times with 1 mL of ice-cold PBS and subsequently treated with trypsin-EDTA at 37 °C for 3 min to detach the cells as well as remove the surface-bound (noninternalized) protein from the cell membrane. Cells were collected and centrifuged (PR-J centrifuge, International Equipment Company, Nashville, TN) at 1500 rpm for 3 min to separate intracellular (cell pellet) from surface bound (supernatant) fractions. The cell pellet was washed twice with ice-cold PBS and then dissolved in 1 mL of 1 N NaOH. The ^{125}I-proteins were detected using a γ-counter (Packard, Downers Grove, IL), and total cell protein was determined by performing the micro-BCA assay with a Pierce micro-BCA assay kit (Thermo Fisher Scientific, Rockford, IL).

Peptides Preparation and Circular Dichroism Spectroscopy. In order to study the structure changes of the HE-fused CPP peptides under various pH conditions without the interference by GST protein domain, $(HE)_{10}$-$YG(RG)_6$, $(HE)_{10}$-YGR_6G_6, and $(HE)_{10}$-Tat were isolated from the respective GST-fusion proteins by on column thrombin cleavage during GST agarose chromatography. After cleavage, the GST-free peptides were purified using HisPur Ni-NTA resins and dialyzed against 10 mM phosphate buffer followed by Tricine-SDS-PAGE analysis and sterilization by filtration (0.22 μm micropore membrane). The peptide concentrations were determined by their absorption at 280 nm (UV 160U spectrophotometer, Shimadzu, Japan). For CD analysis, peptides were diluted to 25 mM in PBS at different pH ranging from 6.0 to 7.5. A J-815 CD spectrometer equipped with a PTC-423S/15 Peltier thermostatic cell holder (Jasco, Easton, MD) was utilized to measure the spectra.[27] All spectra were recorded from 250 to 160 nm in a 10 mm quartz cuvette at 20 °C using a 0.5 nm data interval and a scanning speed of 100 nm/min. The CD spectra were plotted as an average ellipticity (mdeg) versus wavelength λ (nm).

Statistical Analysis. All data are given as mean ± standard deviation (SD). Mean and SD values were calculated from three independent measurements per treatment group. The Student's t test was exploited to perform comparison between data sets, where statistically significant differences were assigned for P values of <0.05.

RESULTS

Expression and Purification of Recombinant GST-Fusion Protein. Plasmids encoding GST-$(HE)_n$-CPP were successfully constructed in pGEX-4T-1 vector (Figure 1A) according to the positive sequencing results. Recombinant GST-fusion proteins were expressed in *E. coli* BL-21 and purified by GSH affinity chromatography. Expression and purification was confirmed by Coomassie blue-stained SDS-PAGE, where gel of purified GST-$(HE)_n$-$YG(RG)_6$ (Figure 1B) and GST-$(HE)_n$-YGR_6G_6 (Figure 1C), n = 8, 10 and 12, showed gradient positions with varied HE repeats and approximately 90% purity based on the band densities. The yield of each protein obtained from 500 mL LB culture (Table 1) indicated that prolonging HE-repeats in the oligopeptide sequence decreased expression yield.

Cell Uptake and Surface Binding Study. To investigate the impact of the length of HE repeats on the pH sensitivity of CPP-incorporated recombinant GST-fusion proteins, cellular uptake and surface binding assay were performed. Confluent HeLa cell monolayers were grown in 6-well plates and treated with ^{125}I-radiolabeled proteins in serum-free RPMI 1640 media,

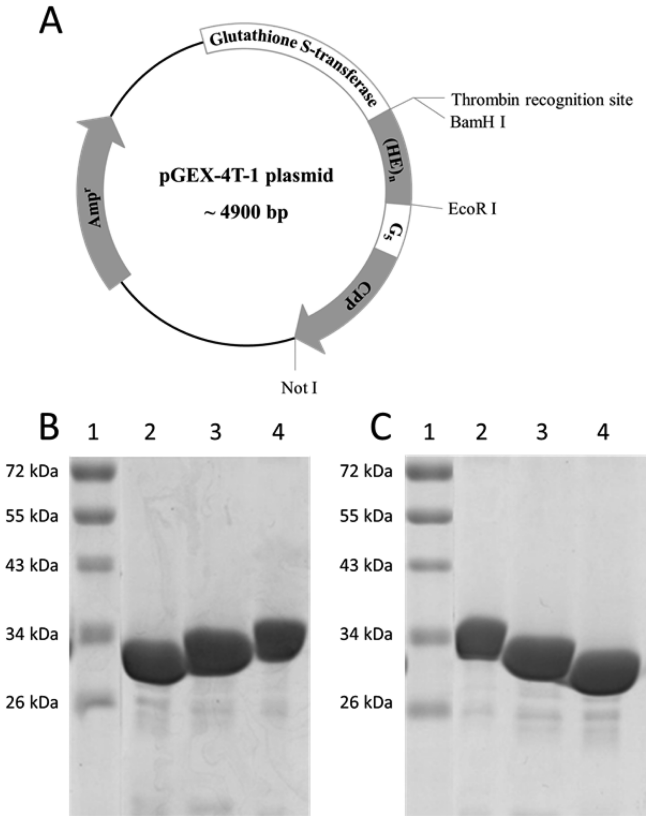

Figure 1. Design and production of recombinant GST-fusion protein. (A) Plasmid map of recombinant GST-fusion proteins, where n is equal to 8, 10, or 12 and $YG(RG)_6$ or YGR_6G_6 is used as the CPP. Purified GST-$(HE)_n$-$YG(RG)_6$ (B) and GST-$(HE)_n$-YGR_6G_6 (C) were analyzed by SDS-PAGE followed by Coomassie blue staining. For (B), lane 1: MW marker; lane 2: GST-$(HE)_8$-$YG(RG)_6$; lane 3: GST-$(HE)_{10}$-$YG(RG)_6$; lane 4: GST-$(HE)_{12}$-$YG(RG)_6$. For (C), lane 1: MW marker; lane 2: GST-$(HE)_{12}$-YGR_6G_6; lane 3: GST-$(HE)_{10}$-YGR_6G_6; lane 4: GST-$(HE)_8$-YGR_6G_6.

at various pH (6.0, 6.5, 7.0, and 7.5) for 1 h at 37 °C. The data (Figure 2) demonstrated that incorporation of HE oligopeptide significantly affected cell uptake and surface binding in a pH-dependent manner.

As seen in the cell uptake figures (Figures 2A, C, and E), the internalization of the fusion proteins increased with decreasing pH. The fusion protein with mixed arginine configuration, GST-$(HE)_n$-$YG(RG)_6$, showed a 5-, 4-, and 3-fold increase for n = 8, 10 and 12, respectively, at pH 7.5 vs 6. With a clustered arginine configuration, GST-$(HE)_n$-YGR_6G_6 was more sensitive to pH changes, where a 5-, 6-, and 4 fold increase for n = 8, 10, and 12, respectively, was observed at pH 7.5 vs 6. The different lengths of (HE) repeats also affected the pH-dependent uptake patterns. The fusion proteins with 8 and 10 (HE) repeats showed higher uptake than the 12-(HE) repeat peptide across the entire pH range for both GST-$(HE)_n$-$YG(RG)_6$ and GST-$(HE)_n$-YGR_6G_6. Furthermore, the 12-(HE) repeat peptides showed less of a difference in the clustered vs mixed configuration than the 8- and 10-(HE) repeats. The surface binding of the fusion proteins showed a weaker pH-dependency than the cell uptake, where a 2-fold difference was noted at pH 7.5 vs 6 for all fusion proteins tested (Figures 2B, D, and F). As a control, the cell uptake and surface binding of GST-$(HE)_{10}$ was also measured. The results shown in Figure

dx.doi.org/10.1021/mp400747k | *Mol. Pharmaceutics* 2014, 11, 1583−1590

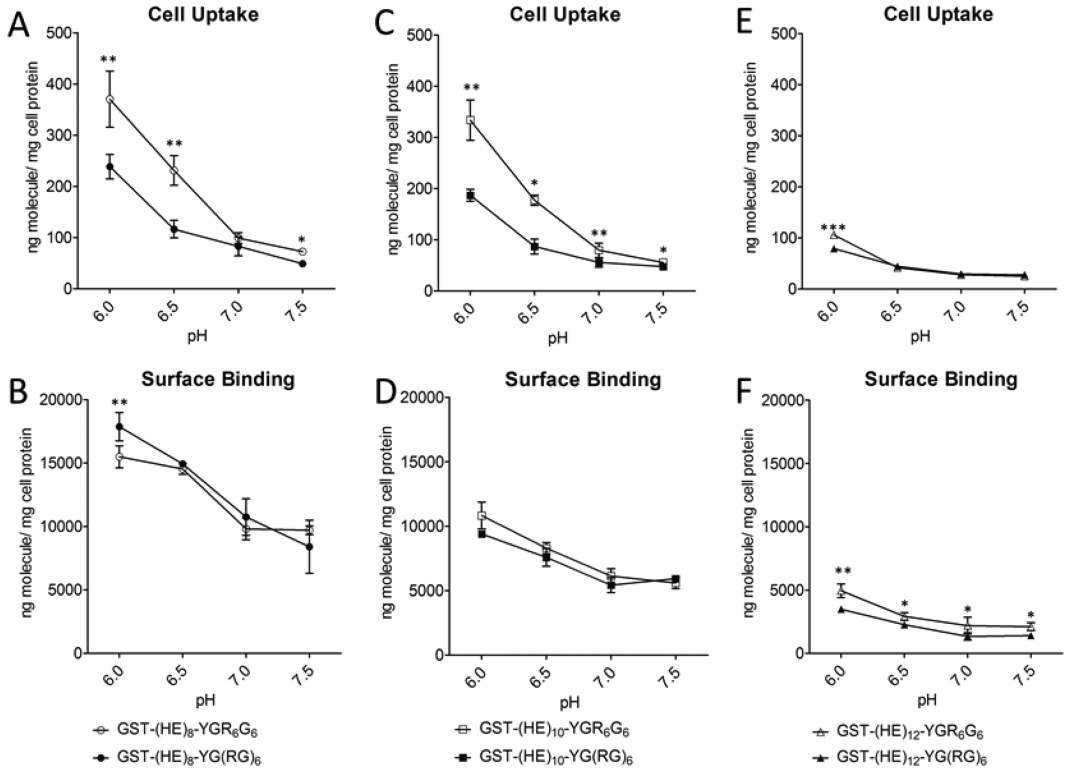

Figure 2. The influence of HE oligopeptide on cell uptake and surface binding in HeLa cells at diverse pH. HeLa cell monolayers were treated with 5 μg/mL ^{125}I-GST-$(HE)_n$-CPP for 1 h at 37 °C at pH 6.0, 6.5, 7.0, and 7.5, where n is equal to 8, 10, or 12 and CPP is $YG(RG)_6$ or YGR_6G_6. Cell uptake and surface binding were determined as described in the Experimental Section. All data were normalized by total cell protein, that is, nanograms per milligram of cell protein, and presented as averages ± standard deviation from three independent measurements per condition. Cell uptake (A) and surface binding (B) of ^{125}I-GST-$(HE)_8$-$YG(RG)_6$ and ^{125}I-GST-$(HE)_8$-YGR_6G_6; cell uptake (C) and surface binding (D) of ^{125}I-GST-$(HE)_{10}$-$YG(RG)_6$ and ^{125}I-GST-$(HE)_{10}$-YGR_6G_6; cell uptake (E) and surface binding (F) of ^{125}I-GST-$(HE)_{12}$-$YG(RG)_6$ and ^{125}I-GST-$(HE)_{12}$-YGR_6G_6. Asterisk represents statistically significant differences in cellular uptake or surface binding at diverse pH between CPPs in the same group (*, $p < 0.05$; **, $p < 0.01$; ***, $p < 0.001$).

3 indicate that both binding and uptake of GST-$(HE)_{10}$ was not dependent on pH, and was low across the pH range tested.

Comparison with Tat[47−57]. Cell-penetrating Tat[47−57] peptide is one of the most extensively studied CPPs. The cell internalization and binding of GST-$(HE)_{12}$-Tat was compared to the blocked oligoarginine construct at a ∼1:1.5 ratio of cationic amino acids in the CPP sequence (R, K) to number of (HE) repeats (i.e., GST-$(HE)_{12}$-Tat vs GST-$(HE)_{10}$-YGR_6G_6). In the cell experiments (Figure 4), GST-$(HE)_{12}$-Tat exhibited a stronger pH sensitivity in both cell uptake (4.4-fold increase at pH 6.0 versus pH 7.5) and surface binding (2.0-fold increase at pH 6.0 versus pH 7.5). Therefore, the pH sensitivity was comparable to the arginine in a clustered configuration, which is consistent with the Tat peptide sequence.

Influence of Serum on Cell Uptake and Surface Binding. To mimic physiological conditions, FBS was added in the media at different concentrations from 1−10%, and the cell uptake and surface binding were assayed at pH 6.0 and 7.5. As expected, the surface binding and uptake of both GST-$(HE)_{10}$-YGR_6G_6 and GST-$(HE)_{10}$-$YG(RG)_6$ decreased with increasing concentrations of FBS (Figures 5 and 6). However, the ratio of either the surface binding or uptake at pH 6.0 versus 7.5 was similar in the presence of 1−10% FBS (Table 2). Therefore, serum did not affect the pH sensitivity of the constructs.

Circular Dichroism Spectroscopy. The secondary structure of the HE-peptides was analyzed by CD spectroscopy.[28−31] As shown in Figures 7B and 8, $(HE)_{10}$-YGR_6G_6 and $(HE)_{10}$-Tat exhibited a random-coiled structure with a minimum at 198 nm. The $(HE)_{10}$-$YG(RG)_6$ peptide, on the other hand, exhibited a β-sheet conformation with a minimum at 218 nm and maximum at 195 nm (Figure 7A). The content of β-sheet conformation $(HE)_{10}$-$YG(RG)_6$ was evaluated at various pH, and the β-sheet content increased with increasing pH. The CD spectra showed an isosbestic point at 205 nm, consistent with a two-state transition from random coil to β-sheet. For both for $(HE)_{10}$-YGR_6G_6 and $(HE)_{10}$-Tat, pH had limited influence on the secondary structure (Figure 8).

■ DISCUSSION

It is well established that positively charged amino acid residues, that is, arginine and lysine, are essential for both the binding and uptake of CPPs in mammalian cells. However, the polycationic charge is also responsible for the nonspecific cellular interaction and, consequently, the cytotoxicity of CPPs that limits the *in vivo* application in drug delivery. Therefore, the reversible masking of the positive charge has been a promising approach to avoid the nonspecific binding of CPPs to cell surface. In this report, we used oligoarginine peptides, with arginyl residues in a clustered (i.e., YGR_6G_6) or a mixed (i.e., $YG(RG)_6$) configuration, as the CPP models to investigate the influence of the negative charges generated from a pH-dependent anionic HE oligopeptide on the binding and uptake of CPP in cultured HeLa cells.

Due to the number of glutamic acid residues, a longer HE oligopeptide should provide a higher masking efficiency, which

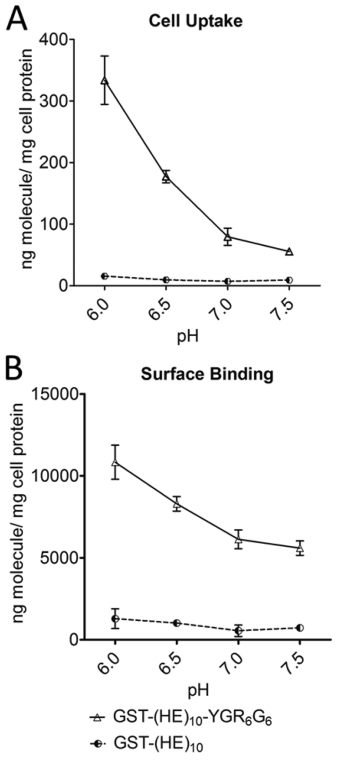

Figure 3. Comparison of cell uptake (A) and surface binding (B) between GST-$(HE)_{10}$-YGR_6G_6 (open triangle) and GST-$(HE)_{10}$ (black/white circle) in HeLa cells at diverse pH. HeLa cell monolayers were treated with 5 μg/mL ^{125}I-GST-$(HE)_{10}$-YGR_6G_6 or ^{125}I-GST-$(HE)_{10}$ for 1 h at 37 °C at pH 6.0, 6.5, 7.0, and 7.5. Cell uptake and surface binding were determined as described in the Experimental Section. All data were normalized by total cell protein and are presented as averages ± standard deviation from three independent measurements per condition.

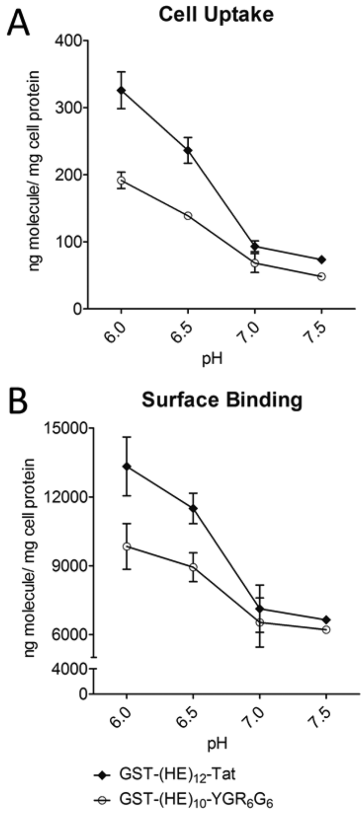

Figure 4. Comparison of cell uptake (A) and surface binding (B) between GST-$(HE)_{10}$-YGR_6G_6 (open circle) and GST-$(HE)_{12}$-Tat (closed diamond) in HeLa cells at diverse pH. Upon confluence, HeLa cell monolayers were incubated with 5 μg/mL ^{125}I-GST-$(HE)_{10}$-YGR_6G_6 and ^{125}I-GST-$(HE)_{12}$-Tat for 1h at 37 °C at pH 6.0, 6.5, 7.0, and 7.5. Cell uptake and surface binding were determined as described in the Experimental Section. All data were normalized by total cell protein, and presented as averages ± standard deviation from three independent measurements per condition.

should yield a lower cellular binding of the CPP. In our preliminary studies, we found that oligopeptides with a ~1:1 ratio of HE-to-cationic amino acid (R/K) showed a lack of masking effect at pH 7.5, with lower pH sensitivity. Therefore, in this study, an excess of negative charges in HE repeats was designed to ensure a complete neutralization of the six positive charges in $YG(RG)_6$ or YGR_6G_6 at pH 7.5. As shown in Figure 2E, both $YG(RG)_6$- and YGR_6G_6-fused proteins showed a decrease in cell uptake and surface binding with an increase of the length of HE oligopeptide. When linked to a 12-mer HE oligopeptide, the cell absorption capacity of $YG(RG)_6$ and YGR_6G_6 was immensely restrained, leading to a minimal cell uptake and a poor pH sensitivity in the pH range from 7.5 to 6.5 (Figure 2E). Although GST-$(HE)_8$-YGR_6G_6 showed the highest uptake, GST-$(HE)_{10}$-YGR_6G_6 actually had the greatest pH sensitivity among the three proteins (5-, 6-, and 4-fold increase for HE n = 8, 10, and 12 at pH 7.5 vs 6.0). Moreover, nonspecific uptake and binding of GST-$(HE)_{10}$-YGR_6G_6 were lower than GST-$(HE)_8$-YGR_6G_6 at pH 7.5. Thus, the 10-mer (HE) repeat showed the optimal pH sensitivity and low binding at neutral pH.

From the cellular uptake assay (Figures 2A, C, and E), the internalization of GST-$(HE)_n$-$YG(RG)_6$ showed only a moderate increase with the decrease in pH from 7.0 to 6.0. On the other hand, a much sharper increase of cell uptake was observed in GST-$(HE)_n$-YGR_6G_6 profiles, with a nearly linear increase from pH 7.0 to 6.0 for GST-$(HE)_8$-YGR_6G_6 and GST-$(HE)_{10}$-YGR_6G_6 and a shift of the pH sensitivity of cellular uptake to lower pH for GST-$(HE)_{12}$-YGR_6G_6. This result in pH sensitivity is consistent with the estimated pI of $(HE)_n$-YGR_6G_6 fused oligopeptides (Table 1). Although $(HE)_n$-$YG(RG)_6$ and $(HE)_n$-YGR_6G_6 had a similar pI with n = 8, 10, or 12, they exhibited a totally different pH-dependent profile in cellular internalization. The different profile is possibly due to the different interaction patterns between HE and CPP with either clustered or mixed positive charges. However, regardless of the length of HE oligopeptide moiety, all three fusion peptides with YGR_6G_6 showed a significantly higher cell uptake at pH 6 than that of their $YG(RG)_6$ counterpart. At pH 6.5 (i.e., pH = pK_a for histidine), half of the anionic charges in HE peptide will have been neutralized by the protonated histidyl residues, which, according to our data, is sufficient to begin to recover the binding and uptake of the CPP sequence. The significantly higher cellular uptake of clustered Arg-peptide than that of mixed Arg-peptide at pH 6.5 or lower is possibly due to the fact that the insertion of glycine residues between the arginine residues will result in a decreased cell uptake of the oligoarginine.[25] However, the difference in cell uptake between these two HE fusion peptides, especially at pH 6.5, appeared much greater than that what has been observed between YGR_6G_6 and $YG(RG)_6$. It is likely that the difference is also due to the presence of $(HE)_n$ sequence in the fusion oligopeptides

dx.doi.org/10.1021/mp400747k | Mol. Pharmaceutics 2014, 11, 1583−1590

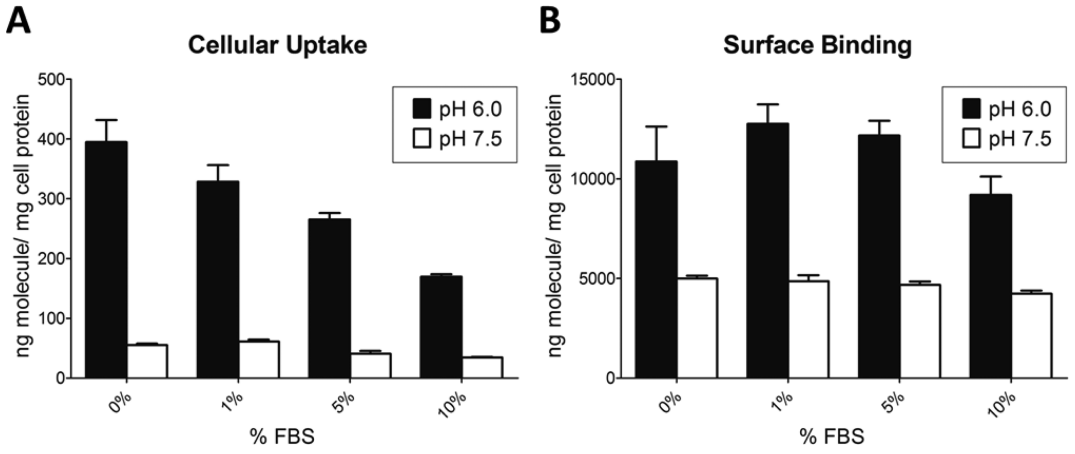

Figure 5. The effect of serum on cell uptake (A) and surface biding (B) of GST-$(HE)_{10}$-YGR_6G_6 in Hela cells at pH 7.5 (open bars) and 6.0 (closed bars). HeLa cell monolayers were incubated in medium containing 5 μg/mL ^{125}I-GST-$(HE)_{10}$-YGR_6G_6 in the presence of 0%, 1%, 5%, or 10% FBS for 1 h at 37 °C. Cell uptake and surface binding were determined as described in the Experimental Section. All data were normalized by total cell protein and presented as averages ± standard deviation from three independent measurements per condition.

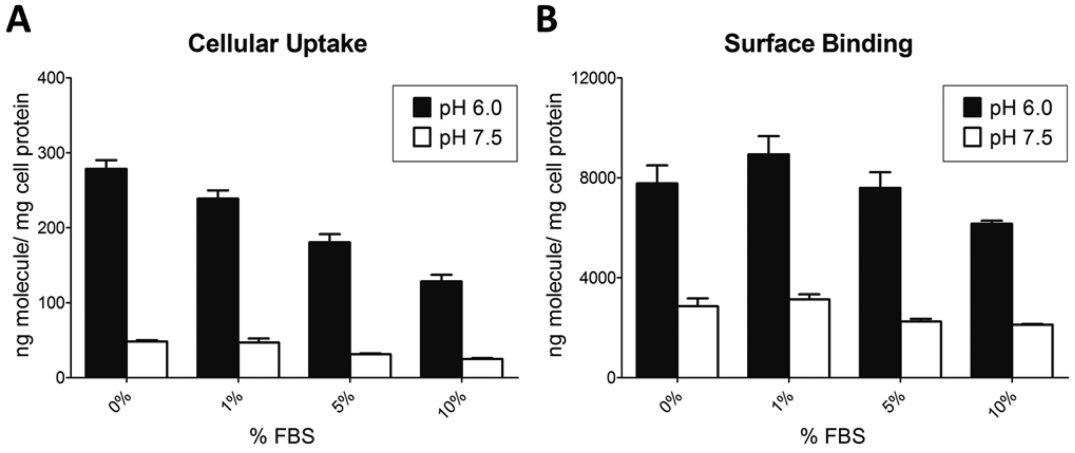

Figure 6. The effect of serum on cell uptake (A) and surface biding (B) of GST-$(HE)_{10}$-$YG(RG)_6$ in HeLa cells at pH 7.5 (open bars) and 6.0 (closed bars). HeLa cell monolayers were incubated in medium containing 5 μg/mL ^{125}I-GST-$(HE)_{10}$-$YG(RG)_6$ in the presence of 0%, 1%, 5%, or 10% FBS for 1 h at 37 °C. Cell uptake and surface binding were determined as described in the Experimental Section. All data were normalized by total cell protein and presented as averages ± standard deviation from three independent measurements per condition.

Table 2. Effect of Serum on pH Sensitivity of GST-Fusion Proteins

		ratio (pH 6.0/pH 7.5)[a]	
sequence	% FBS	cell uptake	surface binding
GST-$(HE)_{10}$-R_6G_6	0%	7.2	2.2
	1%	5.4[b]	2.6
	5%	6.5	2.6
	10%	4.9[b]	2.2
GST-$(HE)_{10}$-$(RG)_6$	0%	5.8	2.7
	1%	5.1	2.8
	5%	5.8	3.4
	10%	5.1	2.9

[a]Ratios were calculated based on the results shown in Figures 5 and 6. [b]Indicates a statistically significant difference (p = 0.03) compared to the ratio in the respective 0% FBS control. All other differences compared to the respective 0% FBS controls were nonsignificant (p > 0.05).

which may influence the overall conformation of the fusion peptides. Therefore, the difference in conformation between $(HE)_{10}$-YGR_6G_6 and $(HE)_{10}$-$YG(RG)_6$ was further investigated by using CD spectroscopy.

In order to further evaluate the oligopeptides for further use in *in vivo* studies, the pH sensitivity was evaluated *in vitro* in the presence of FBS. As shown in Figures 5 and 6, increasing amounts of FBS led to decreased cell uptake and binding. This result was expected because the addition of FBS has been shown to decrease the nonspecific binding and the electrostatic adsorption of CPPs.[32,33] However, the presence of up to 10% FBS did not affect the pH sensitivity of the constructs because the ratio of cell uptake and of surface binding at pH 6.0 versus pH 7.5 was similar across the 0−10% FBS range (Table 2).

CD spectra have been studied on some arginine-rich peptides with cluster of arginine residues, that is, HIV-1 Tat,[34,35] R_7,[35] and R_9,[34,36] to assess their secondary structures. However, no evidence showed that they have an ordered structure regardless of solvent/buffer systems used in those studies. As shown in Figure 7B, $(HE)_{10}$-YGR_6G_6 tends to have an unstructured conformation in the range from pH 6.0 to 7.5, with a minimum absorption around 198 nm and no positive peak.[36,37] However, the spectra of $(HE)_{10}$-$YG(RG)_6$, as shown in Figure 7A, indicated an antiparallel β-sheet conformation,[28] whereas its

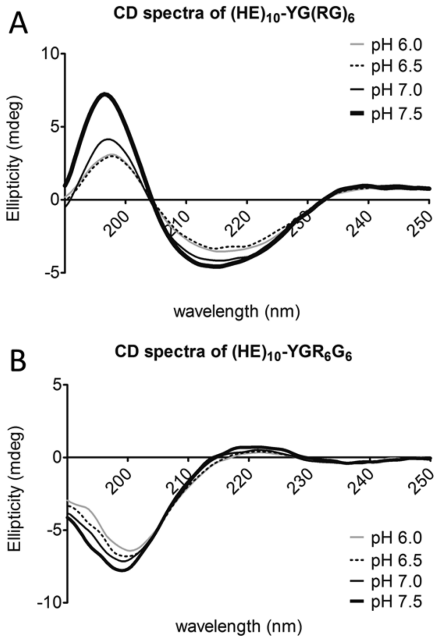

Figure 7. Circular dichroism (CD) spectra of $(HE)_{10}$-$YG(RG)_6$ (A) and $(HE)_{10}$-YGR_6G_6 (B) at pH 6.0 (gray line), 6.5 (long dashed black line), 7.0 (regular black line), and 7.5 (bold black line). $(HE)_{10}$-$YG(RG)_6$ and $(HE)_{10}$-YGR_6G_6 were isolated from their corresponding recombinant GST-fusion proteins, GST-$(HE)_{10}$-$YG(RG)_6$ and GST-$(HE)_{10}$-YGR_6G_6, after overnight thrombin treatment. After buffer exchange and desalting, isolated peptides were diluted to 25 mM in 10 mM phosphate buffer saline (PBS). CD spectra were determined as described in the Experimental Section. Data were plotted as ellipticity (mdeg) versus wavelength (nm) after deduction of background.

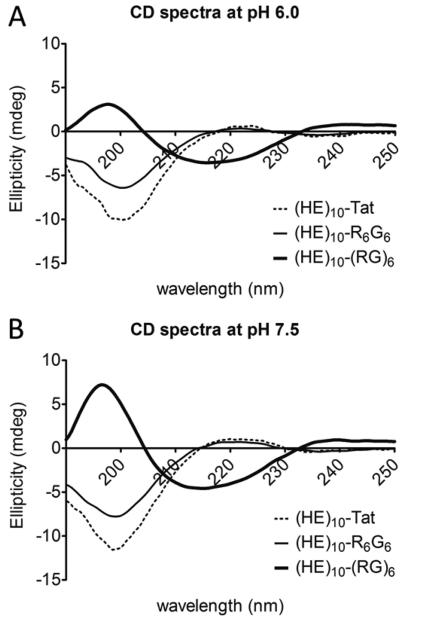

Figure 8. Circular dichroism (CD) spectra of $(HE)_{10}$-$YG(RG)_6$ (bold line), $(HE)_{10}$-YGR_6G_6 (regular line) and $(HE)_{10}$-Tat (long dashed line) at pH 6.0 (A) and 7.5 (B). GST-$(HE)_{10}$-$YG(RG)_6$, GST-$(HE)_{10}$-YGR_6G_6, and GST-$(HE)_{10}$-Tat were treated with thrombin for 18 h. Next morning, $(HE)_{10}$-$YG(RG)_6$, $(HE)_{10}$-YGR_6G_6, and $(HE)_{10}$-Tat could be eluted from corresponding GSH columns with PBS with or without 250 mM acetate. Buffer exchange and desalting were then performed. Afterward, isolated peptides were diluted in 10 mM PBS at a final concentration of 25 mM. CD spectra were determined as described in the Experimental Section. Data were plotted as ellipticity (mdeg) versus wavelength (nm) after deduction of background.

secondary structural content varied in different pH environments. Because the CD measurements were obtained from isolated HE-CPP peptides without GST, the drastic difference in the spectra between $(HE)_{10}$-YGR_6G_6 and $(HE)_{10}$-$YG(RG)_6$ as shown in Figure 7A clearly suggests a difference in the structure of these 2 peptides. Glycine is the most conformationally unrestrained amino acid, and it has been utilized between Arg to form a β-hairpin conformation by other groups.[38] In our study, the insertion of glycine as a spacer between arginine residues to create an alternating RG sequence, that is, $(RG)_6$, will most likely facilitate the electrostatic interaction between the guanidine group of arginine residues in the CPP-sequence and the carboxylic group of glutamic acid residue in the HE-sequence. In addition, the stability of the ionic pairing may be also responsible for the adoption and maintenance of an antiparallel β-sheet conformation of $(HE)_n$-$YG(RG)_6$ fusion peptides.[39] Figure 7A shows that the majority of $(HE)_{10}$-$YG(RG)_6$ still adopts the same conformation even at pH 6.0, that is, when the net charge of the $(HE)_{10}$ moiety in the fusion peptide is only slightly anionic (net charge = −2). Consequently, the maintenance of the antiparallel β-sheet conformation at mildly acidic pH condition may stabilize the HE-oligoarginine complex resulting in the poor pH sensitivity of $(HE)_n$-$YG(RG)_6$. The conformational dependence of pH sensitivity of $(HE)_n$-fused CPPs is consistent with our finding with HE-Tat[47−57] oligopeptide. Tat[47−57] consists of clusters of 6 Arg and 2 Lys residues and is one of the most well-studied CPPs. When fused with $(HE)_{12}$, the fusion peptide showed a high pH sensitivity between pH 7.0 to pH 6.0 in cell uptake and binding assay (Figures 4A and 4B).

In conclusion, our results indicate that HE oligopeptide can be conjugated to CPPs with both clustered and mixed positive charges to form CPP derivatives with a reactivation in mildly acidic environment. However, a higher pH sensitivity can be expected in clustered than in mixed positive charge CPPs. In general, the increase of the length of the HE-repeat can decrease the nonspecific absorption of CPP at neutral pH, but it will also decrease the reactivation at acidic pH. Therefore, when designing a reversible masking polyanion to decrease the nonspecific binding of CPPs in drug delivery across biological barriers, both the total charges of the anions and the molecular conformation of the ionic complex should be considered.

AUTHOR INFORMATION

Corresponding Authors

*J. L. Zaro. Tel.: +1 323 442 1902. Fax: +1 323 442 1390. E-mail: zaro@usc.edu. Address: 1985 Zonal Ave, Los Angeles, CA 90033, United States.

*J. Tu. E-mail: jiashengtu@aliyun.com.

Notes

The authors declare no competing financial interest.

ACKNOWLEDGMENTS

This work was supported by grants (to J.L.Z.) from the NIH National Cancer Institute, R21 CA169841, and the University of Southern California (USC) Ming Hsieh Institute for Research of Engineering-Medicine for Cancer. C.S. is a visiting graduate student at USC from China Pharmaceutical University (CPU). He would like to express his appreciation and gratitude to China Scholarship Council (CSC) for providing financial

support to allow him working on his Ph.D. dissertation research at USC.

REFERENCES

(1) Frankel, A. D.; Pabo, C. O. Cellular uptake of the tat protein from human immunodeficiency virus. *Cell* **1988**, *55* (6), 1189−93.
(2) Kenien, R.; Zaro, J. L.; Shen, W. C. MAP-mediated nuclear delivery of a cargo protein. *J. Drug Target* **2012**, *20* (4), 329−37.
(3) Zaro, J. L.; Shen, W. C. Cytosolic delivery of a p16-peptide oligoarginine conjugate for inhibiting proliferation of MCF7 cells. *J. Controlled Release* **2005**, *108* (2−3), 409−17.
(4) Mo, R. H.; Zaro, J. L.; Shen, W. C. Comparison of cationic and amphipathic cell penetrating peptides for siRNA delivery and efficacy. *Mol. Pharm.* **2012**, *9* (2), 299−309.
(5) Eguchi, A.; Akuta, T.; Okuyama, H.; Senda, T.; Yokoi, H.; Inokuchi, H.; Fujita, S.; Hayakawa, T.; Takeda, K.; Hasegawa, M.; Nakanishi, M. Protein transduction domain of HIV-1 Tat protein promotes efficient delivery of DNA into mammalian cells. *J. Biol. Chem.* **2001**, *276* (28), 26204−10.
(6) Liu, B. R.; Huang, Y. W.; Winiarz, J. G.; Chiang, H. J.; Lee, H. J. Intracellular delivery of quantum dots mediated by a histidine- and arginine-rich HR9 cell-penetrating peptide through the direct membrane translocation mechanism. *Biomaterials* **2011**, *32* (13), 3520−37.
(7) Saw, P. E.; Ko, Y. T.; Jon, S. Efficient Liposomal Nanocarrier-mediated Oligodeoxynucleotide Delivery Involving Dual Use of a Cell-Penetrating Peptide as a Packaging and Intracellular Delivery Agent. *Macromol. Rapid Commun.* **2010**, *31* (13), 1155−62.
(8) Lee, E. S.; Gao, Z.; Kim, D.; Park, K.; Kwon, I. C.; Bae, Y. H. Super pH-sensitive multifunctional polymeric micelle for tumor pH(e) specific TAT exposure and multidrug resistance. *J. Controlled Release* **2008**, *129* (3), 228−36.
(9) Kamei, N.; Morishita, M.; Eda, Y.; Ida, N.; Nishio, R.; Takayama, K. Usefulness of cell-penetrating peptides to improve intestinal insulin absorption. *J. Controlled Release* **2008**, *132* (1), 21−5.
(10) Kamei, N.; Morishita, M.; Ehara, J.; Takayama, K. Permeation characteristics of oligoarginine through intestinal epithelium and its usefulness for intestinal peptide drug delivery. *J. Controlled Release* **2008**, *131* (2), 94−9.
(11) Kanazawa, T.; Taki, H.; Tanaka, K.; Takashima, Y.; Okada, H. Cell-penetrating peptide-modified block copolymer micelles promote direct brain delivery via intranasal administration. *Pharm. Res.* **2011**, *28* (9), 2130−9.
(12) Koren, E.; Torchilin, V. P. Cell-penetrating peptides: breaking through to the other side. *Trends Mol. Med.* **2012**, *18* (7), 385−93.
(13) MacEwan, S. R.; Chilkoti, A. Harnessing the power of cell-penetrating peptides: activatable carriers for targeting systemic delivery of cancer therapeutics and imaging agents. *Wiley Interdiscip. Rev.: Nanomed. Nanobiotechnol.* **2013**, *5* (1), 31−48.
(14) Patel, L. N.; Zaro, J. L.; Shen, W. C. Cell penetrating peptides: intracellular pathways and pharmaceutical perspectives. *Pharm. Res.* **2007**, *24* (11), 1977−92.
(15) Richard, J. P.; Melikov, K.; Vives, E.; Ramos, C.; Verbeure, B.; Gait, M. J.; Chernomordik, L. V.; Lebleu, B. Cell-penetrating peptides. A reevaluation of the mechanism of cellular uptake. *J. Biol. Chem.* **2003**, *278* (1), 585−90.
(16) Olson, E. S.; Aguilera, T. A.; Jiang, T.; Ellies, L. G.; Nguyen, Q. T.; Wong, E. H.; Gross, L. A.; Tsien, R. Y. In vivo characterization of activatable cell penetrating peptides for targeting protease activity in cancer. *Integr. Biol.* **2009**, *1* (5−6), 382−93.
(17) Shamay, Y.; Adar, L.; Ashkenasy, G.; David, A. Light induced drug delivery into cancer cells. *Biomaterials* **2011**, *32* (5), 1377−86.
(18) Sethuraman, V. A.; Bae, Y. H. TAT peptide-based micelle system for potential active targeting of anti-cancer agents to acidic solid tumors. *J. Controlled Release* **2007**, *118* (2), 216−24.
(19) Zaro, J. L.; Fei, L.; Shen, W. C. Recombinant peptide constructs for targeted cell penetrating peptide-mediated delivery. *J. Controlled Release* **2012**, *158* (3), 357−61.
(20) Fei, L.; Yap, L. P.; Conti, P. S.; Shen, W. C.; Zaro, J. L. Tumor targeting of a cell penetrating peptide by fusing with a pH-sensitive histidine-glutamate co-oligopeptide. *Biomaterials* **2014**, 4082−4087.
(21) Mukherjee, S.; Ghosh, R. N.; Maxfield, F. R. Endocytosis. *Physiol. Rev.* **1997**, *77* (3), 759−803.
(22) Bryant, R. E.; Rashad, A. L.; Mazza, J. A.; Hammond, D. beta-Lactamase activity in human pus. *J. Infect. Dis.* **1980**, *142* (4), 594−601.
(23) Zaro, J. L.; Vekich, J. E.; Tran, T.; Shen, W. C. Nuclear localization of cell-penetrating peptides is dependent on endocytosis rather than cytosolic delivery in CHO cells. *Mol. Pharm.* **2009**, *6* (2), 337−44.
(24) Eiriksdottir, E.; Konate, K.; Langel, U.; Divita, G.; Deshayes, S. Secondary structure of cell-penetrating peptides controls membrane interaction and insertion. *Biochim. Biophys. Acta* **2010**, *1798* (6), 1119−28.
(25) Fei, L.; Ren, L.; Zaro, J. L.; Shen, W. C. The influence of net charge and charge distribution on cellular uptake and cytosolic localization of arginine-rich peptides. *J. Drug Target* **2011**, *19* (8), 675−80.
(26) Sonoda, S.; Schlamowitz, M. Studies of 125I trace labeling of immunoglobulin G by chloramine-T. *Immunochemistry* **1970**, *7* (11), 885−98.
(27) Greenfield, N. J. Using circular dichroism spectra to estimate protein secondary structure. *Nat. Protoc.* **2006**, *1* (6), 2876−90.
(28) Greenfield, N.; Fasman, G. D. Computed circular dichroism spectra for the evaluation of protein conformation. *Biochemistry* **1969**, *8* (10), 4108−16.
(29) Kelly, S. M.; Jess, T. J.; Price, N. C. How to study proteins by circular dichroism. *Biochim. Biophys. Acta* **2005**, *1751* (2), 119−39.
(30) Holzwarth, G.; Doty, P. The Ultraviolet Circular Dichroism of Polypeptides. *J. Am. Chem. Soc.* **1965**, *87*, 218−28.
(31) Venyaminov, S.; Baikalov, I. A.; Shen, Z. M.; Wu, C. S.; Yang, J. T. Circular dichroic analysis of denatured proteins: inclusion of denatured proteins in the reference set. *Anal. Biochem.* **1993**, *214* (1), 17−24.
(32) Moulton, H. M.; Nelson, M. H.; Hatlevig, S. A.; Reddy, M. T.; Iversen, P. L. Cellular uptake of antisense morpholino oligomers conjugated to arginine-rich peptides. *Bioconjugate Chem.* **2004**, *15* (2), 290−9.
(33) Kosuge, M.; Takeuchi, T.; Nakase, I.; Jones, A. T.; Futaki, S. Cellular internalization and distribution of arginine-rich peptides as a function of extracellular peptide concentration, serum, and plasma membrane associated proteoglycans. *Bioconjugate Chem.* **2008**, *19* (3), 656−64.
(34) Futaki, S.; Suzuki, T.; Ohashi, W.; Yagami, T.; Tanaka, S.; Ueda, K.; Sugiura, Y. Arginine-rich peptides. An abundant source of membrane-permeable peptides having potential as carriers for intracellular protein delivery. *J. Biol. Chem.* **2001**, *276* (8), 5836−40.
(35) Thoren, P. E.; Persson, D.; Esbjorner, E. K.; Goksor, M.; Lincoln, P.; Norden, B. Membrane binding and translocation of cell-penetrating peptides. *Biochemistry* **2004**, *43* (12), 3471−89.
(36) Liu, B. R.; Lo, S. Y.; Liu, C. C.; Chyan, C. L.; Huang, Y. W.; Aronstam, R. S.; Lee, H. J. Endocytic Trafficking of Nanoparticles Delivered by Cell-penetrating Peptides Composed of Nona-arginine and a Penetration Accelerating Sequence. *PLoS One* **2013**, *8* (6), e67100.
(37) Kelly, S. M.; Price, N. C. The use of circular dichroism in the investigation of protein structure and function. *Curr. Protein Pept. Sci.* **2000**, *1* (4), 349−84.
(38) Ramirez-Alvarado, M.; Kortemme, T.; Blanco, F. J.; Serrano, L. Beta-hairpin and beta-sheet formation in designed linear peptides. *Bioorg. Med. Chem.* **1999**, *7* (1), 93−103.
(39) de Alba, E.; Blanco, F. J.; Jimenez, M. A.; Rico, M.; Nieto, J. L. Interactions responsible for the pH dependence of the beta-hairpin conformational population formed by a designed linear peptide. *Eur. J. Biochem.* **1995**, *233* (1), 283−92.
(40) Protein Calculator v3.4. http://www.scripps.edu/~cdputnam/protcalc.html (accessed Jan 2014).